

# Fluorination of Single-Wall Carbon Nanotubes and Subsequent Derivatization Reactions

VALERY N. KHABASHESKU,\*  
W. EDWARD BILLUPS, AND  
JOHN L. MARGRAVE\*

*Rice Quantum Institute and Center for Nanoscale Science and Technology, Department of Chemistry, Rice University, Houston, Texas 77005-1892*

Received June 17, 2002

## ABSTRACT

This Account focuses on the most recent and systematic efforts in the area of functionalization chemistry of the single-wall carbon nanotubes (SWNTs) which utilizes direct fluorination for the preparation of "fluoronanotubes" and their subsequent derivatization. The results obtained prove that the addition of fluorine drastically enhances the reactivity of the nanotube side walls. The use of this strategy as a versatile tool for preparation and manipulation of SWNTs with variable side-wall functionalities has been demonstrated. The functionalized SWNTs have shown an improved solubility in selected solvents and significantly altered electrical, mechanical, and optical properties. An overview of new synthetic methods for preparation and a discussion of characterization data for the functionalized SWNTs are provided.

## Introduction

Since their discovery by Iijima in 1991,<sup>1</sup> carbon nanotubes have become the subject of intense research activity worldwide. The unique mechanical, optical, and electronic properties and other phenomena exhibited by carbon nanotubes offer many opportunities for their applications.<sup>2–5</sup> Single-wall carbon nanotubes (SWNTs), in particular, possess a remarkable tensile strength and, depending on their diameter and helicity, can be metallic,

semiconducting, or insulating as well as chiral or achiral. The uses of nanotubes for fabrication of reinforced fibers and nanocomposites,<sup>6</sup> field-emission displays,<sup>7</sup> and nano-size probe tips for atomic force microscopy<sup>8</sup> and their capability of hydrogen storage<sup>9</sup> are being investigated extensively. For these and many other novel applications, the separation of individual SWNTs from their bundles is becoming essential. This would improve the dispersion and solubilization of the SWNTs in common organic solvents and/or water, which is needed for their processing and manipulation.

Chemical functionalization by the attachment of various functional groups to SWNTs was shown to be efficient in breaking the nanotube bundles and giving soluble samples.<sup>10</sup> Besides improving the solubility and processibility, functionalization opens an opportunity for altering the structural and electronic properties of SWNTs and affords new types of nanotube-based materials with useful properties of their own. Chemical functionalizations of the nanotube ends are not suitable for these purposes since they bring only a highly localized transformation of the SWNT electronic structure and do not change the bulk properties of these materials. These functionalizations have been most extensively explored through the oxidation of SWNTs and have been shown to form shortened nanotubes with carboxylic acid groups at the ends, which have been further derivatized by reactions with thionyl chloride and long-chain amines<sup>8,10,11</sup> or by esterification.<sup>12,13</sup>

By comparison, side-wall functionalization naturally results in a very significant modification of the intrinsic properties of SWNTs. The challenges faced in this type of chemical modification of SWNTs are related to the necessity for nondestructive attachment of functional groups to the graphene walls in order to preserve the tubular structure, and also to the fact that SWNTs are not very reactive, in part due to a much lower curvature of the nanotube walls [e.g., in (10,10) SWNTs] than in fullerenes, which exhibit rich chemistry.<sup>2</sup> Therefore, appropriate choices of reagents and experimental conditions become decisive. Direct side-wall attachments of hydrogen via Birch reduction,<sup>14</sup> aryl groups,<sup>15,16</sup> nitrenes, carbenes, and radicals<sup>17</sup> as well as 1,3-dipolar additions<sup>18</sup> to the SWNTs have been reported. In this Account, we will focus on our

Valery N. Khabashesku received his M.Sc. in chemistry from Moscow State University (USSR) in 1973, followed by a Ph.D. (1980) and a D.Sc. (Prof. Dr., 1998) in organic chemistry from the Zelinsky Institute of Organic Chemistry of the Russian Academy of Sciences (Moscow). In 1990–1991, he was a Visiting Scientist with the U.S. National Academy of Sciences, performing collaborative research at the University of Texas, Austin, and the University of Colorado, Boulder, in the laboratory of Prof. J. Michl. He is a recipient of a 2001 State Prize of the Russian Federation in Science and Engineering for his extensive work on the chemistry of low-coordinated silicon, germanium, and tin, shared with his colleagues. Currently, he is a Faculty Fellow in the Department of Chemistry at Rice University and also holds joint appointment as a Principal Scientist at the Zelinsky Institute. His research interests include chemistry and applications of carbon and heterocarbon nanomaterials, high-pressure–high-temperature synthesis, and matrix isolation spectroscopy of transient molecules.

W. Edward Billups received his B.S. (1961) and M.S. (1965) in chemistry from Marshall University in Huntington, WV, followed by a Ph.D. in chemistry from Pennsylvania State University in 1970. That same year he joined the faculty at Rice University, where he has been Professor of Chemistry since 1981. He served as a Chairman of the Chemistry Department from 1985 to 1991. His research interests include the chemistry of small ring systems, reactive intermediates, synthetic methods, organo-transition metal chemistry, the chemistry of free metal atoms, fullerene chemistry, and the chemistry of carbon nanotubes.

John L. Margrave received his B.S. in engineering physics (1948) and Ph.D. in Chemistry (1950) from the University of Kansas, Lawrence. After working as an AEC Postdoctoral Fellow from 1951 to 1952 at UC Berkeley, he joined the faculty at the Chemistry Department of University of Wisconsin, where he advanced through the ranks from Instructor to Professor of Chemistry (1960). He moved to Rice University in 1963 and served as a Chairman of the Chemistry Department, Dean for Advanced Studies, and Vice President for Advanced Studies and Research. In 1986 he became E. D. Butcher Professor of Chemistry. He also was a Director of the Materials Research Center and a Vice President for Research at the Houston Advanced Research Center, where he currently is Chief Scientific Officer. He is also a Visiting Professor at Texas Southern University. In 1974 he was elected to membership in the U.S. National Academy of Science. He has received ACS Awards in Inorganic and Fluorine Chemistry, two IR-100 Awards, and has just been selected for a 2002 Chemical Pioneer Award of the American Institute of Chemists. His current research areas involve physical and inorganic chemistry, fluorine chemistry, high-temperature–high-pressure phenomena, nanoscience, and environmental chemistry.

most recent results on functionalization chemistry of SWNTs which utilizes direct fluorination for the preparation of “fluoronanotubes” and their subsequent derivatization as a versatile tool for preparation and manipulation of nanotubes with variable side-wall functionalities. Progress in the bulk synthesis and purification of SWNTs, achieved by Smalley and co-workers<sup>19–22</sup> at Rice University, has made large quantities of the high-quality samples available for this work.

## Fluoronanotubes

**Preparation.** Fluorinated SWNTs (fluoronanotubes) have been prepared by direct fluorination of both laser-ablated graphite-grown carbon nanotubes (L-SWNTs)<sup>19,20</sup> and those produced by a high-pressure CO disproportionation process (HiPco-SWNTs),<sup>21,22</sup> using the technology developed earlier in our laboratories for the fluorination of graphite.<sup>23</sup> Extensive fluorination studies<sup>24</sup> were carried out to establish optimal conditions (reaction temperatures, reaction times, addition of HF catalyst) to reach a saturation stoichiometry (nearly C<sub>2</sub>F) without destruction of the tube structure. It was also found that the degree of fluorination depends on the residual metal content from catalysts used in the purified SWNTs and the conditions of preparation and treatment of the buckypaper samples (nature of solvent, annealing temperature) prior to fluorination.

The fluorination of L-SWNT buckypaper, prebaked at 1100 °C in a vacuum, was carried out at temperatures ranging from 150 to 600 °C. IR spectroscopy (KBr pellet method) confirmed the presence of covalently bound fluorine (peaks of the C–F stretches in the 1220–1250 cm<sup>-1</sup> region) in the samples fluorinated in the absence of HF catalyst at temperatures of 250 °C and higher, and not for those fluorinated at 150 °C. Transmission electron microscopy (TEM) images indicate that the tube structures remain largely intact under treatment at temperatures as high as 325 °C, yielding approximately C<sub>2</sub>F product bulk composition according to electron probe microanalysis (EPMA). The SWNTs are essentially all destroyed (i.e., “unzipped”) when fluorinated at 400 °C and above to form a fluorographite and some multiwall carbon nanotube-like material. As a result of the side-wall functionalization of the SWNTs by fluorine, the electrical properties of the fluoronanotubes differ dramatically from those of pristine SWNTs. Fluoronanotubes, prepared by fluorination at temperatures of 250 °C and above, are insulators (two-point resistance across the length of buckypaper sample > 20 MΩ), while the pristine nanotubes are good conductors (two-point resistance 10–15 Ω).<sup>24a</sup>

With the addition of HF, which is a known catalyst for fluorination of graphite, the saturated C/F ratio (~2) for the L-SWNT tube structure was reached at a lower reaction temperature (250 °C) while maintaining the same reaction time (~5 h). The other observed effect of HF addition was a noticeable upshift of the C–F stretching frequency in the attenuated total reflectance–Fourier transform infrared (ATR-FTIR) spectra of fluoronanotubes

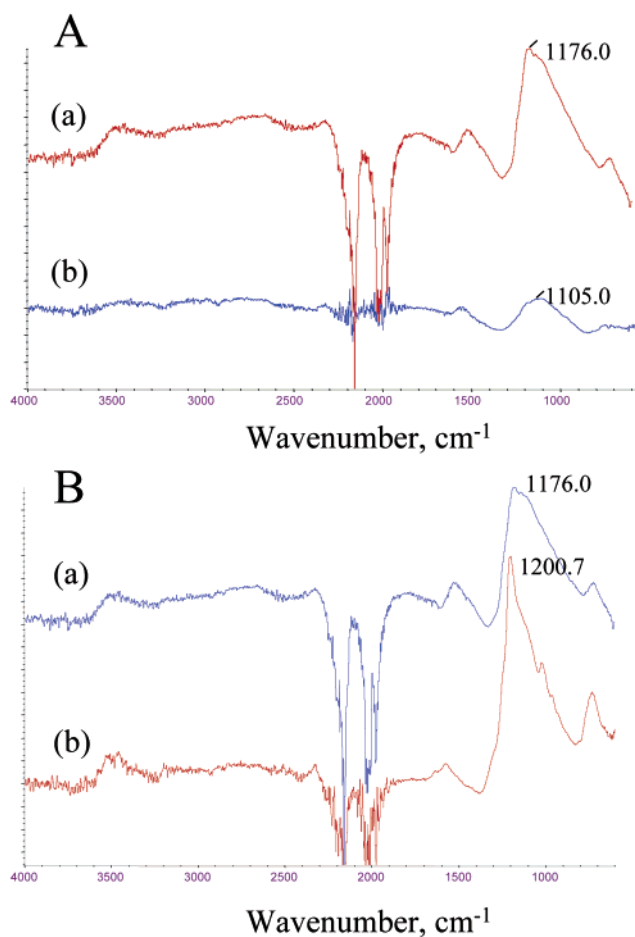


**FIGURE 1.** ATR-FTIR spectra of L-SWNTs: (A) fluorinated at 200 °C with HF addition (a) and without HF addition (b); (B) fluorinated at 200 °C (a) and at 250 °C (b). Negative absorptions at 2000 and 2200 cm<sup>-1</sup> are due to the diamond crystal of the ATR accessory.

(Figure 1A), which indicated the formation of more covalent and therefore stronger C–F bonds. The same upshifting effect and a higher relative intensity of the C–F band in the IR spectra were also seen when the fluorination temperature was raised (Figure 1B). These phenomena are in agreement with those observed earlier for fluorinated graphite.<sup>23</sup>

The HiPco-SWNTs have smaller average diameters (~1 nm for the (8,8) nanotubes) than L-SWNTs (~1.38 nm, corresponding to the (10,10) tubes) and, therefore, due to a higher curvature are more reactive. This is particularly indicated by the observation that, under the same fluorination conditions, more fluorine can be attached onto the side walls of HiPco-SWNTs.<sup>24</sup> For instance, in the presence of HF, the near C<sub>2</sub>F composition for the tubular structure of the HiPco-SWNTs has been produced at a fluorination temperature as low as 150 °C, while under the same conditions the L-SWNTs yielded fluoronanotubes with a significantly lower fluorine content (C/F ratio higher than 3).

**Solvation Properties.** Fluoronanotubes are shown to form metastable solutions in DMF, THF, and alcohols after sonication. They do not dissolve in perfluorinated solvents as well as in water, diethylamine, and acetic acid. The

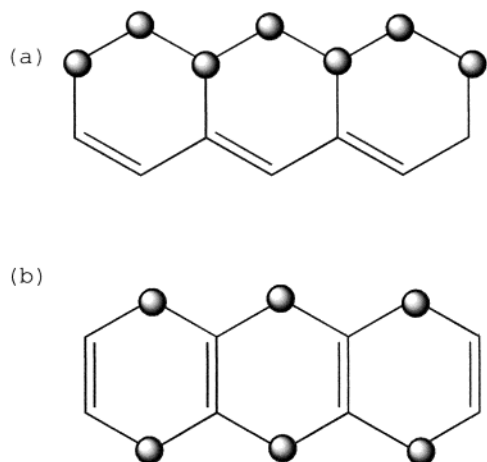


**FIGURE 2.** Proposed fluorine addition patterns on the fluoronanotubes: 1,2-addition (a) and 1,4-addition (b).

solvation of individual (“unroped”) fluoronanotubes was verified by dispersing them on a mica substrate and examining them with atomic force microscopy (AFM).<sup>25</sup> The solutions in alcohols were stable for a few days to over a week. Among the series of alcohols studied, 2-propanol and 2-butanol were found to be the best solvents. A likely scenario for such solvation would be hydrogen bonding between the hydroxyl hydrogen in alcohol and the nanotube-bound fluorine:  $R-O-H \cdots F-(C_nF)$ . This bonding is likely facilitated by an increased ionic nature of the C–F bond in fluoronanotubes, in contrast with alkyl fluorides, in which, according to the recent studies, the fluorine is suggested to be a poor hydrogen bond acceptor.<sup>26</sup> X-ray photoelectron spectroscopy (XPS) analysis of fluorinated SWNTs supports the idea of a more ionic fluorine bonded in fluoronanotubes by revealing an F 1s peak at a binding energy of 687 eV, located at a much lower binding energy than the F 1s peak in poly(tetrafluoroethylene) (691.5 eV).

**Structural and Mechanistic Considerations.** Insight into the possible fluoronanotube structures has been provided by molecular modeling calculations and scanning tunneling microscopy (STM) imaging.<sup>27</sup> On the basis of the experimentally established limiting  $C_2F$  stoichiometry at which fluorinated tubes can still maintain their tubular structure,<sup>24a,b</sup> two isomeric structures, resulting from fluorine addition to either 1,2 or 1,4 positions within a hexagonal ring on the graphene-like side wall of the nanotube, have been proposed (Figure 2). Due to the arrangement of the  $\pi$ -bonds, the 1,2-isomer can be conducting through an electron flow along the conjugated bonds parallel to tube axis, whereas the 1,4-isomer, with its isolated double bonds, will yield insulating fluoronanotubes. From molecular mechanics (MM+)<sup>24c</sup> and semiempirical (AM1 and CNDO)<sup>27</sup> calculations, it was found that the 1,4-isomer is more stable, although the energy difference between the two isomers is quite small (only 1 kcal/mol per F atom). Higher level calculations on fluorinated armchair (10,10) SWNTs of  $C_2F$  stoichiometry using density functional theory (PBE/3 and LSDA/3-21G) and periodic boundary conditions revealed that, on the con-

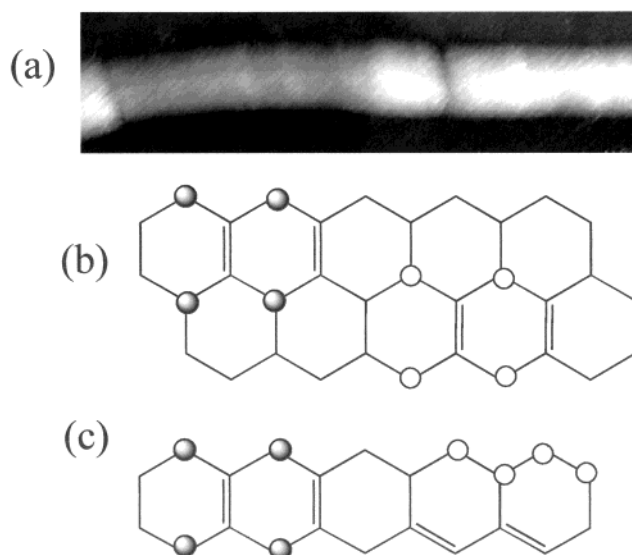


**FIGURE 3.** STM image of an individual fluoronanotube (a). Modeling of observed gap formation in STM images: (b) multiple fluorination initiation sites and (c) mixture of both 1,2- and 1,4-additions.

trary, the 1,2-isomer is more stable than the 1,4-isomer; however, the total energy difference is again fairly small (about 4 kcal/mol per  $C_2F$  unit).<sup>28</sup> Given such small differences in energies between these two isomers, calculated at various levels of theory, and in the absence of the developed separation procedures, it is reasonable to assume that both isomers coexist in the fluoronanotube material.

The STM images show that the fluorinated regions typically form bands around the circumference of the tube (Figure 3a). This may imply that the addition of fluorine to the side wall of the pristine SWNT should occur more favorably around the circumference of the tube. Nevertheless, AM calculations indicate that addition along the axis of the tube for the 1,2-isomer is about 30 kcal/mol more exothermic than circumferential 1,2-addition, while in the case of the 1,4-isomer the addition around the circumference of the tube is approximately 10 kcal/mol more energetically favorable than propagation along the tube axis.<sup>24c,27</sup> On that basis, the origination of the abrupt band boundaries, observed in the STM images of fluoronanotubes (even those having the saturated  $C_2F$  stoichiometry), could be explained by a circumferential addition mechanism proceeding via initiation of the 1,4-isomer at multiple sites along the tube and propagating on alternate pairs of rows (Figure 3b). However, since the calculated energy difference between the 1,2- and 1,4-isomers is small, one can also expect the possibility of having both types of fluorine addition occur simultaneously during the fluorination process to form discrete isomeric domains on the nanotube (Figure 3c). Various defects in the side-wall graphene structure might also play important roles in either initiating or terminating such domains.

**Pyrolysis for Nanotube Cutting.** Examination of the products of thermal decomposition of  $C_2F$  fluoronanotubes in vacuo at temperatures of up to 800 °C by variable-temperature pyrolysis–electron ionization mass spec-

trometry (VTP-EIMS) revealed the following species:  $\text{CF}_3^+$  ( $m/z = 69$ ),  $\text{C}_3\text{F}_5^+$  ( $m/z = 131$ ),  $\text{C}_3\text{F}_7^+$  ( $m/z = 169$ ), and  $\text{C}_4\text{F}_7^+$  ( $m/z = 181$ ).<sup>24b</sup> These data indicate that the pyrolysis of fluoronanotubes is dominated by formation of volatile carbon–fluorine-containing molecules and not simply by the loss of elementary fluorine. Along with the observation of the extended dark bands in the STM images of the partially fluorinated SWNTs  $\text{C}_n\text{F}$  ( $n > 2$ ) due to bare nanotube side walls, these results have led to the idea of using fluorination followed by pyrolysis as chemical “scissors” for cutting the nanotubes. Very recently, Gu et al.<sup>29</sup> demonstrated a process which involves the fluorination of catalyst-free HiPco-SWNTs to a stoichiometry of  $\text{C}_5\text{F}$ , followed by pyrolysis at temperatures up to 1000 °C in an argon atmosphere that results in cutting the nanotubes at the fluorinated sites to short lengths (20–200 nm). When the pyrolysis process was monitored in situ with thermogravimetric analysis (TGA)-FTIR, the fluorine was shown to be driven from the fluoronanotube structure as  $\text{CF}_4$  and  $\text{COF}_2$  (due to oxygen covalently attached to the SWNT side wall during the first steps of the purification procedure<sup>30</sup>). The cut SWNTs were characterized by Raman spectra, TGA data, and AFM images showing their drastically shortened lengths in comparison with the pristine SWNTs (Figure 4). Studies of the cut SWNTs are now in progress for potential applications including chemically assisted assembly, gas adsorbants, drug delivery vehicles, and polymer composite reinforcements.

### Chemical Derivatization of Fluoronanotubes

Recent density functional theory (DFT) calculations of the electronic densities of states have shown that the Fermi energy of the fluoronanotubes is considerably shifted toward lower values compared to that of the pristine SWNTs. The conduction bands are energetically lowered as well.<sup>28</sup> This implies that the fluoronanotubes are better electron acceptors than the bare carbon nanotubes, and therefore they should more eagerly interact with strong nucleophilic reagents as well as undergo reduction to bare SWNTs by alkali metals. These chemical reactions are also facilitated by the fact that the C–F bonds in fluoronanotubes, as in fluorinated fullerenes, are weakened relative to the C–F bonds in alkyl fluorides owing to an eclipsing strain effect,<sup>31,32</sup> and thus fluorine could be more easily displaced. The unique electronic structure and improved solubility of fluoronanotubes and the weaker C–F bond have opened a door to the chemical syntheses of a wide variety of side-wall-functionalized nanotubes with interesting properties using fluoronanotubes as precursors.

**Reactions with Organolithium Reagents.** We have demonstrated that alkyllithium reagents can be used to attach alkyl groups to the side walls of the nanotubes.<sup>24c,33</sup> The reactions have been carried out by adding the RLi (R = methyl, *n*-butyl, *tert*-butyl, *n*-hexyl, phenyl) reagent to the fluoronanotubes, dispersed in THF, ether, or hexane, at –40 °C followed by sonication for 10 min and stirring at room temperature overnight under argon. After completion of the workup procedure,<sup>24c</sup> the final products were

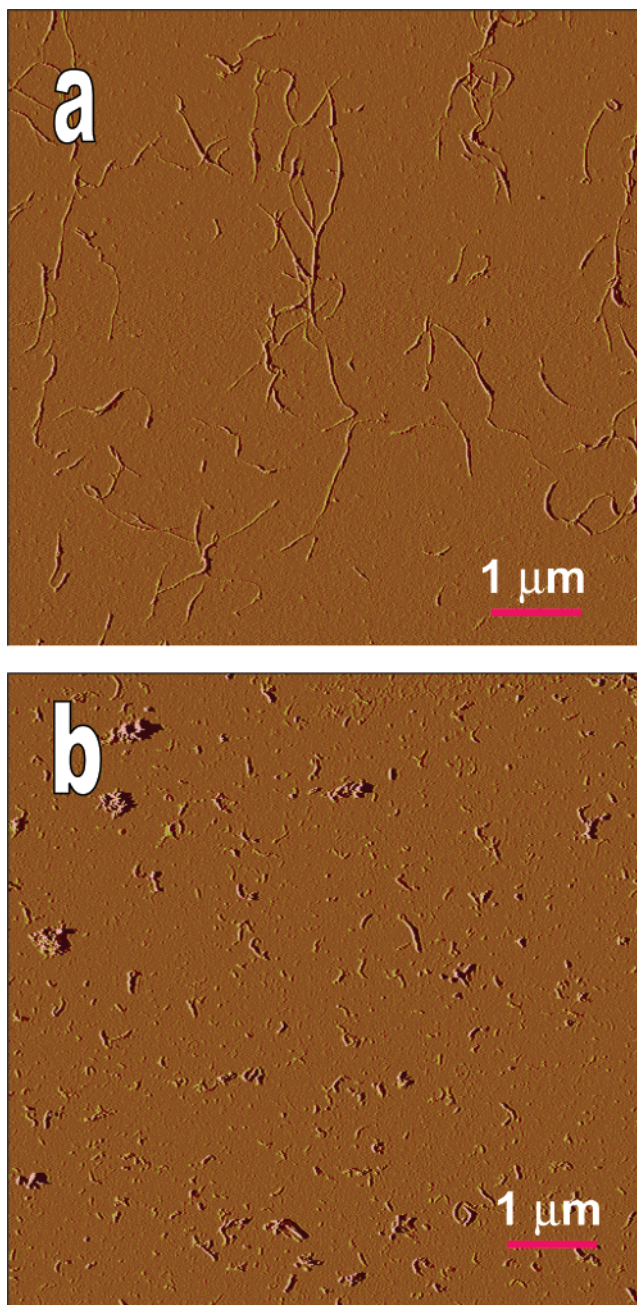


FIGURE 4. AFM images of (a) micrometer-scale length SWNTs and (b) nanometer-scale length SWNTs produced by chemical “cutting”.

dried in a vacuum oven and then characterized by ATR-FTIR, UV-Vis-NIR, TGA, and TGA-FTIR techniques.

The alkylated SWNTs have shown in the ATR-FTIR spectra (Figure 5) the typical alkyl groups’ C–H stretching and deformation absorptions in the 2850–2970 and 1000–1470  $\text{cm}^{-1}$  regions, respectively, as well as a peak at about 1580  $\text{cm}^{-1}$  due to an activated C=C stretching mode. The observed absence of the van Hove electronic transition features in the UV-Vis-NIR spectra supports the occurrence of the side-wall functionalization which dramatically alters the electronic structure of alkylated nanotubes with respect to the pristine SWNTs. As a result, these alkylated SWNTs are soluble in common organic solvents such as THF and chloroform.

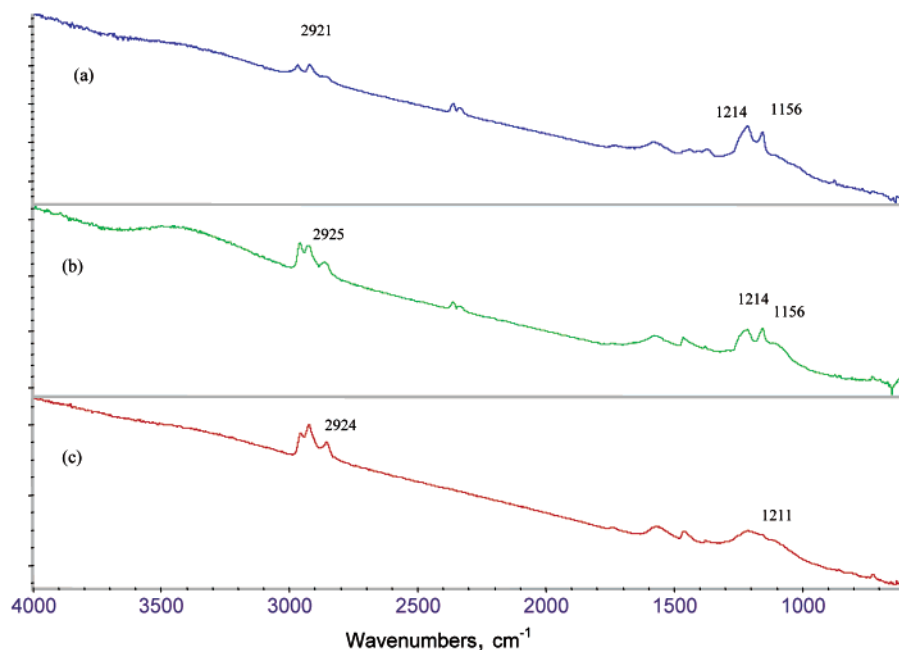


FIGURE 5. ATR-FTIR spectra of alkylated SWNTs: (a) methylated SWNTs, (b) butylated SWNTs, and (c) hexylated SWNTs.

On the basis of the weight loss at 200–450 °C during the TGA runs, the nanotube carbon-to-alkyl ratios were calculated for methyl, *n*-butyl, and *n*-hexyl SWNTs, which indicate that alkylation of the fluorinated HiPco-SWNTs results in a higher degree of functionalization in comparison with the L-SWNTs, in line with the expected enhanced reactivity due to the increased tube curvature. We have obtained the STM images of the side-wall-buty-lated SWNTs, which show that for these derivatives the typical fluoronanotubes' banded morphology is no longer visible. Instead, relatively large ( $\sim 10$  Å) bright spots due to side-wall-attached butyl groups with an average spacing of 50 Å are apparent while scanning along the nanotube.<sup>27</sup>

TGA-FTIR analysis has shown on the derivative plots a single maximum for the methylated and two maxima for the *n*-butylated and *n*-hexylated SWNTs, respectively. These maxima were synchronized by the same peaks on the chemigrams (Figure 6A) of the C–H stretching region in the FTIR spectra of volatile products (Figure 6B), demonstrating the presence of corresponding alkyl groups in the nanotubes and also a likely two-step mechanism for the removal of the alkyl groups, other than methyl. VTP-EIMS studies of the methylated SWNTs have shown that under vacuum conditions the evolution of methyl groups ( $m/z = 15$ ) is maximized at a temperature of about 490 °C, far too high to be due to physisorbed species.<sup>24b</sup> We found that the alkylation of the SWNTs is reversible, since after heating of these materials in Ar at 500 °C a complete recovery of the pristine nanotubes occurred.

Due to steric effects, *tert*-butyllithium did not react effectively, resulting in low alkylation and predominant defluorination of the fluoronanotubes, to yield the product showing van Hove transition bands in the UV-Vis-NIR spectra. Steric effects can also account for more extensive alkylation observed in cases when less sterically demanding alkyllithium reagents, such as methyllithium, were

used. These results are consistent with a multistep process that is initiated by a one-electron transfer to the fluoronanotube from the alkyllithium reagent. Elimination of fluoride from the resulting radical anion would lead to a radical site on the SWNT. Recombination of the alkyl radical with this radical site would result in covalent attachment to the side wall. This step is likely sterically controlled, suggesting that, due to crowding of the attaching groups, not every fluorine can be replaced by a new functionality, e.g., an alkyl group.

**Reactions with Grignard Reagents.** Side-wall alkylations of fluoronanotubes by Grignard reagents (alkylmagnesium bromide) in THF have also been carried out.<sup>34</sup> These reactions were done simply by bath sonication of the fluoronanotube paper in excess Grignard reagent in THF for several hours. The solubility of hexylated SWNTs in chloroform was up to  $\sim 0.6$  g/L, as compared to a maximum concentration of 0.1 g/L of pristine nanotubes needed to form stable suspensions in DMF. After heating in air to 250 °C, pristine SWNTs were recovered from the hexylated derivative, for which the attachment of a hexyl group to about 1 in every 10 side-wall carbon atoms has been calculated on the basis of the weight loss monitored by TGA. The analysis of AFM images before and after the oxidation show that the recovered individual tubes are thinner after oxidation by 2–5 Å. The AFM data also indicate that, unlike the case with partially fluorinated SWNTs, this procedure does not shorten the nanotubes. After removal of the hexyl groups, two-point electrical resistance measurements across the buckypaper showed a drop from 372.5 k $\Omega$  to 144.6  $\Omega$ , a value typical of pristine nanotube papers.

**Reactions with Alkoxides.** The solubility of fluoronanotubes in alcohols prompted their functionalization reactions with alkoxides. For instance, sonication of the fluoronanotubes ( $\sim C_2F$ ) in methanol solution of sodium

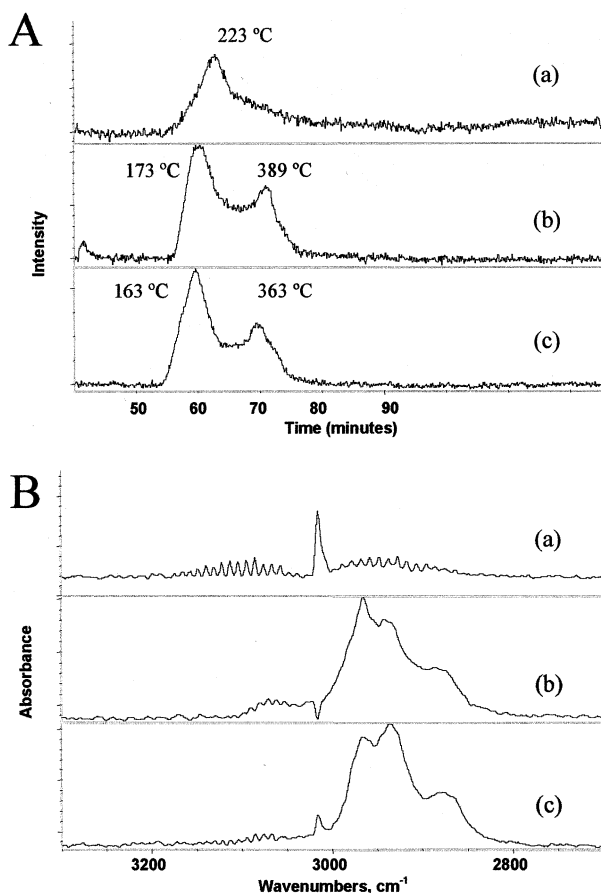


**FIGURE 6.** TGA-FTIR spectra of alkylated SWNTs. (A) Chemigram (intensity vs time) showing peaks due to detachment of alkyl groups, obtained by recording the FTIR spectra in the C–H stretch region. (B) FTIR spectra of species evolving during the time interval from 30 to 80 min. (a) Methylated SWNTs, (b) *n*-butylated SWNTs, and (c) *n*-hexylated SWNTs.

methoxide for 2 h resulted in the formation of methoxy-lated tubes with the suggested stoichiometry of  $C_{4.4}F(OCH_3)_{0.25}$  from EPMA. Thermal degradation studies by VTP-EIMS show that this product loses significant quantities of methoxy groups ( $m/z = 31$ ) at temperatures as high as 650–700 °C. On the basis of these data and the elevated oxygen content shown by the EPMA, the conclusion was made that the methoxy groups are bonded to the nanotube side walls.<sup>24b,26</sup> Recently, functionalizations of fluorinated SWNTs by methoxy, ethoxy, and isopropoxy groups were also done by sonication in lithium hydroxide solutions in methanol, ethanol, and isopropanol, respectively.<sup>35</sup>

**Reactions with Hydrazine and Diamines.** We have shown that the SWNTs, once fluorinated, can be efficiently defluorinated with anhydrous hydrazine via the following reaction,  $4C_nF + N_2H_4 \rightarrow 4C_n + 4HF + N_2$ , done by stirring at room temperature either in neat hydrazine for 1 h or after addition of hydrazine to solutions of fluoronanotubes. EPMA analysis of the solid precipitate yielded a very low fluorine content and no nitrogen, confirming that only defluorination of the SWNTs had occurred.<sup>24,26</sup> Such an outcome of this highly exothermic reaction can be explained by the opportunity to produce (in addition to HF)

the highly thermodynamically stable  $N_2$  molecules. This reaction provides a useful tool for chemical modification of the side walls of the SWNTs, which can be applied for removal of residual fluorine from alkylated fluoronanotubes or for controlled partial defluorination of fluoronanotubes to produce SWNTs with differing fluorine contents and, presumably, different properties.

Unlike the defluorinating action of hydrazine, terminal diamines,  $H_2N(CH_2)_nNH_2$  ( $n = 2, 3, 4, 6$ ), could be used to functionalize SWNTs. The reactions were complete after the fluoronanotubes were refluxed in the corresponding diamine for 3 h in the presence of a catalytic amount of pyridine.<sup>36</sup> Energy-dispersive analysis of X-rays (EDAX) analyses of black precipitates yielded a nitrogen content within 11–16 at. %, and a very low fluorine content (1–2 at. %), suggesting its efficient displacement by the *N*-alkylamino functionalities. TGA-FTIR and VTP-EIMS studies have provided strong evidence for covalent functionalization, showing a major loss of the corresponding attached groups at  $\sim 325$  °C, which were detected, for example, in EIMS by a peak at  $m/z = 59$  ( $HNCH_2CH_2NH_2$ ) in the case of ethylenediamino SWNTs and by peak at  $m/z = 73$  ( $HNCH_2CH_2CH_2NH_2$ ) in the case of propylenediamino SWNTs. TEM images have revealed, in addition to the individual functionalized SWNTs (Figure 7a), an increasing number of the nanotubes cross-linked by the diamino chains, becoming predominant in the case of the larger chain derivatives, hexamethylenediamino SWNTs (Figure 7b). It is interesting that all alkylaminated samples have tested positive by the Kaiser testing procedure for free  $NH_2$  groups. Their availability makes these nanotubes soluble in dilute acids and water and allows them to react, for example, with adipyl chloride to form new “nylon tube” materials or to attach the DNA base to the SWNTs.

**Reactions with Peroxides.** The idea of testing the SWNTs for use as a free radical “sponge” originates from the well-known ability of their fullerene relatives to add a variety of free radicals.<sup>2,37</sup> In our recent work,<sup>38</sup> we have reacted both the pristine and fluorinated HiPco-SWNTs with the organic peroxides, such as lauroyl, benzoyl, *tert*-butyl, and hydrogen peroxides, serving as radical precursors, in attempts to functionalize the nanotube side walls. With the exception of that with lauroyl peroxide, all studied reactions resulted predominantly in formation of side-wall oxidation products. The successful addition of undecyl radicals,  $C_{11}H_{23}$ , generated from lauroyl peroxide, was more efficient in the case of fluoronanotubes than pristine SWNTs, as indicated by a much lower reaction time (3 h vs 5 d) required for observation of prominent C–H stretch peaks in the ATR-FTIR spectra of derivatized tubes (Figure 8a). The covalent attachment of long-chain  $C_{11}H_{23}$  groups to the nanotubes was imaged by TEM (Figure 8b) and confirmed by TGA-FTIR and VTP-EIMS data, indicating the major loss of an undecyl radical and a dimer at a temperature of about 350 °C (peaks in EIMS at  $m/z = 155$  and 310, respectively). The apparent lack of derivatization of the SWNTs by peroxide-generated *tert*-butyl and phenyl radicals is likely due to steric reasons,

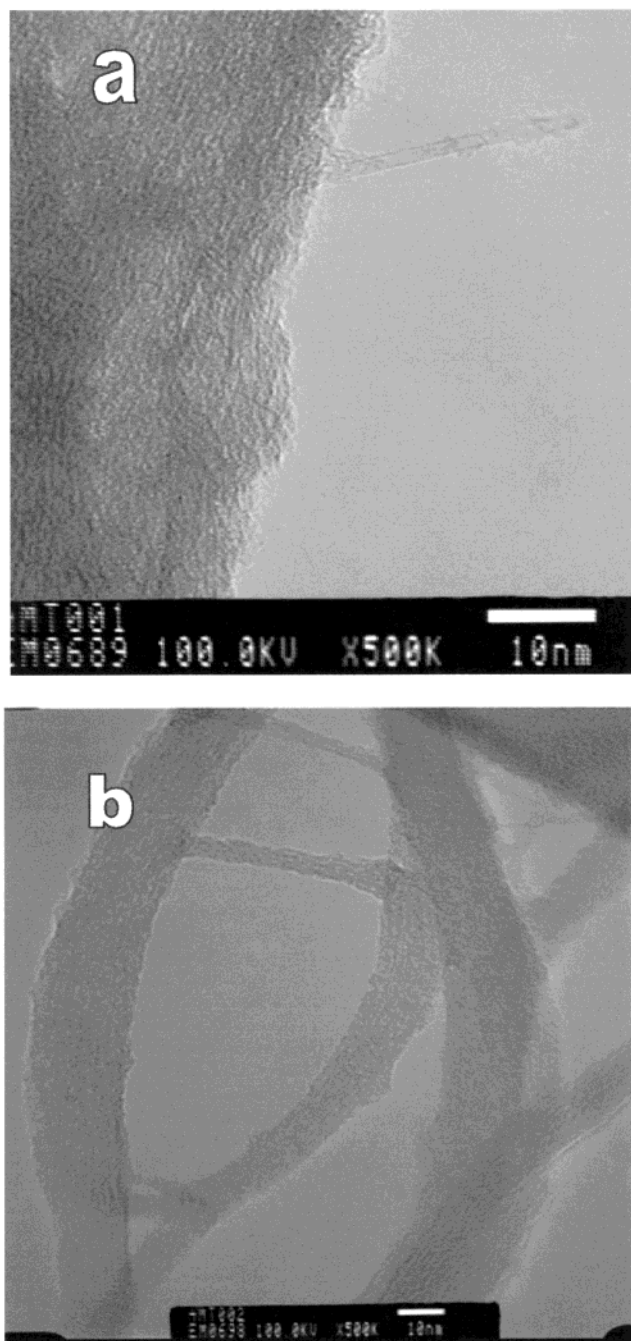


FIGURE 7. TEM images of (a) ethylenediamino-functionalized SWNTs and (b) SWNTs cross-linked by hexamethylenediamine.

as was the case in the unsuccessful attempts to functionalize SWNTs using *tert*-butyl- and phenyllithium reagents.<sup>24c,33</sup>

**Solid-State Inorganic Reactions.** The studies of the solid-state reactions of fluoronanotubes with the series of binary compounds of group VA, VIA, and VIIA elements were prompted by the initial observation of significant reduction of the intensity of the C–F stretch peak in the FTIR spectra of fluorinated SWNTs pressed into KBr pellets as compared to the ATR-FTIR spectra of neat samples.<sup>24c</sup> When a mixture of C<sub>2</sub>F fluoronanotubes was heated with KBr at ~120 °C, the evolution of a reddish gas was observed, and defluorinated SWNTs and KF were formed

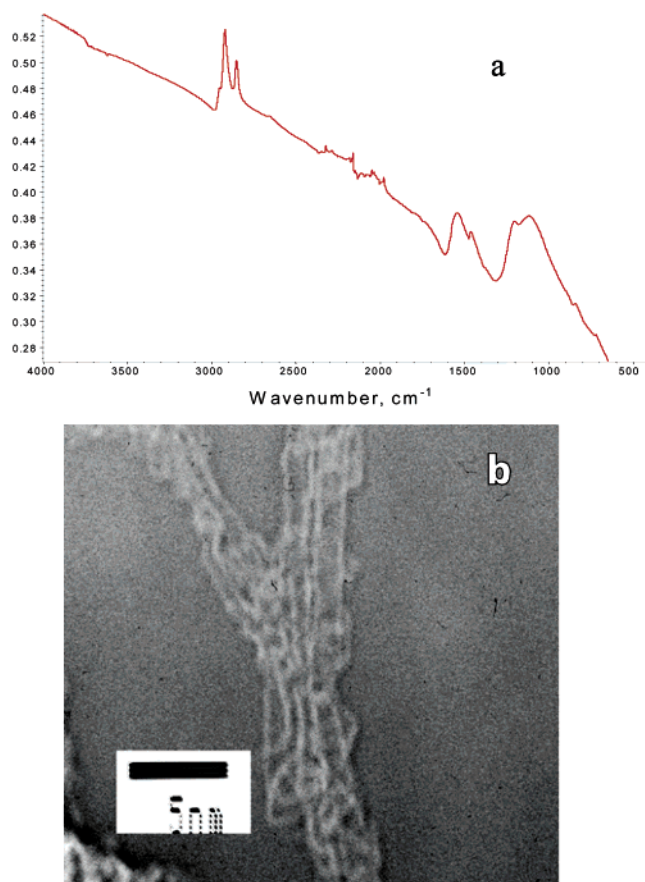


FIGURE 8. Undecyl (C<sub>11</sub>H<sub>23</sub>)-functionalized fluoronanotubes characterized by (a) ATR-FTIR spectrum and (b) TEM image zoomed-in on individual tubes.

according to a reduction–oxidation reaction, (C<sub>2</sub>F)<sub>n</sub> + nKBr → C<sub>2n</sub> + n/2 Br<sub>2</sub> + nKF, as established by the FTIR, Raman, and powder X-ray diffraction (XRD) analyses. The other halides, such as KI, LiI, LiBr, and LiCl, have caused similar transformations, while NaCl and ZnI<sub>2</sub> produced minor changes.<sup>39</sup> For comparison, fluorinated C<sub>60</sub> also reacts as an oxidant, releasing fluorine substantially during heating with KBr, while the fluorographite fluorine remains attached to graphite carbons under the same experimental conditions due to the much stronger C–F bonds.<sup>24c</sup> Among the metal compounds of group VA and VIA elements studied, the sulfide anion in lithium sulfide is oxidized to elemental sulfur by the fluoronanotubes at room temperature, while in the case of zinc sulfide prolonged heating (24 h) at 100 °C was required. The oxides, Li<sub>2</sub>O, FeO, PbO, and MnO, did not react, even at 200 °C, while lithium peroxide reacted at room temperature to form LiF, O<sub>2</sub>, and defluorinated SWNTs. The fluorination of aluminum phosphide by fluoronanotubes to form aluminum trifluoride also took place at room temperature, while a redox reaction with lithium nitride, yielding LiF and N<sub>2</sub>, proceeded at 200 °C. These results indicate that the efficiency of redox reactions of the fluoronanotubes studied is most likely influenced by a combination of two factors: (i) the electronegativity of group VA, VIA, and VIIA elements and (ii) the thermodynamic stability of the metal fluoride products to be

formed. This explains the mild conditions required for these reaction to proceed in the case of lithium halides and a sulfide, and aluminum phosphide, containing the least electronegative elements and producing the most stable fluoride salts,  $\text{AlF}_3$  and  $\text{LiF}$ .

Recently,<sup>40</sup> fluoronanotubes,  $\text{C}_2\text{F}$ , were used as cathodes in a lithium electrochemical cell, for which the discharging performance via a solid-state redox reaction,  $\text{C}_2\text{F} + \text{Li} \rightarrow \text{C}_2 + \text{LiF}$ , has been studied. This cell was found to produce a higher cell potential than that produced by a commercially used fluorographite  $\text{CF}_x$  cell; however, it lasted a shorter time, consistent with the lower fluorine content and a weaker C–F bonds in the fluoronanotubes.

## Conclusions

This review of our results shows that the addition of fluorine to the side walls of SWNTs significantly alters their physical properties (electric conductivity, optical properties, and solubility) and dramatically enhances their chemical reactivity. This makes fluoronanotubes unique precursors for various reactions which can produce a spectrum of new side-wall-functionalized nanotubes with many potentially useful properties. The partial fluorination and further pyrolysis of the SWNTs was shown to be an efficient tool for chemical cutting of the nanotubes, producing SWNTs shortened to 20–200 nm lengths with higher rigidity along the nanotube axis and possibly an exposed inner surface. These findings open additional opportunities for the functionalization chemistry and studies of the length-related properties of the cut nanotubes. New results will undoubtedly continue to emerge from this research.

*We gratefully acknowledge the many contributions of our co-workers and collaborators: J. Stevens, I. Tonks, A. Huang, B. McClaine, P. Reverdy, R. Shukla, H. Peng, Z. Gu, Dr. I. W. Chiang, Dr. J. L. Zimmerman, Dr. R. K. Saini, Dr. E. T. Mickelson, Dr. R. H. Hauge, and Prof. R. E. Smalley. This work was supported by the National Science Foundation, The Robert A. Welch Foundation of Texas, and the Texas Advanced Technology Program.*

## References

- Iijima, S. Helical Microtubules of Graphitic Carbon. *Nature* **1991**, *354*, 56.
- Dresselhaus, M. S.; Dresselhaus, G.; Eklund, P. C. *Science of Fullerenes and Carbon Nanotubes*; Academic Press: San Diego, 1996; Vol. 1.
- Saito, R.; Dresselhaus, M. S.; Dresselhaus, G. *Physical Properties of Carbon Nanotubes*; Imperial College Press: London, 1998.
- Odom, T. W.; Huang, J.-L.; Kim, P.; Lieber, C. M. Structure and Electronic Properties of Carbon Nanotubes. *J. Phys. Chem. B* **2000**, *104*, 2794–2809.
- Rao, C. N. R.; Satishkumar, B. C.; Govindaraj, A.; Nath, M. Nanotubes. *ChemPhysChem* **2001**, *2*, 78–105.
- Gong, X.; Liu, J.; Baskaran, S.; Voise, R. D.; Young, J. S. Surfactant-Assisted Processing of Carbon Nanotube/Polymer Composites. *Chem. Mater.* **2000**, *12*, 1049–1052.
- Gao, B.; Yue, G. Z.; Qiu, Q.; Cheng, Y.; Shimodu, H.; Fleming, L.; Zhou, O. Fabrication and Electron Field Emission Properties of Carbon Nanotube Films by Electrophoretic Deposition. *Adv. Mater.* **2001**, *13*, 1770–1773.
- Wong, S. S.; Harper, J. D.; Lansbury, P. T.; Lieber, C. M. Carbon Nanotube Tips: High-Resolution Probes for Imaging Biological Systems. *J. Am. Chem. Soc.* **1998**, *120*, 603–604.
- Liu, C.; Fan, Y. Y.; Liu, M.; Cong, H. T.; Cheng, H. M.; Dresselhaus, M. S. Hydrogen Storage in Single-Walled Carbon Nanotubes at Room Temperature. *Science* **1999**, *286*, 1127–1129.
- Chen, J.; Hamon, M. A.; Hu, H.; Chen, Y.; Rao, A. M.; Eklund, P. C.; Haddon, R. C. Solution Properties of Single-Walled Carbon Nanotubes. *Science* **1998**, *282*, 95–98.
- Hamon, M. A.; Chen, J.; Hu, H.; Chen, Y. S.; Itkis, M. E.; Rao, A. M.; Eklund, P. C.; Haddon, R. C. Dissolution of Single-Walled Carbon Nanotubes. *Adv. Mater.* **1999**, *11*, 834–840.
- Riggs, J. E.; Guo, Z.; Carroll, D. L.; Sun, Y.-P. Strong Luminescence of Solubilized Carbon Nanotubes. *J. Am. Chem. Soc.* **2000**, *122*, 5879–5880.
- Sun, Y.-P.; Huang, W.; Lin, Y.; Fu, K.; Kitaigorodsky, A.; Riddle, L. A.; Yu, Y. J.; Carroll, D. L. Soluble Dendron-Functionalized Carbon Nanotubes: Preparation, Characterization, and Properties. *Chem. Mater.* **2001**, *13*, 2864–2869.
- Pekker, S.; Salvelat, J.-P.; Jakab, E.; Bonard, J.-M.; Forro, L. Hydrogenation of Carbon Nanotubes and Graphite in Liquid Ammonia. *J. Phys. Chem. B* **2001**, *105*, 7938–7943.
- Bahr, J. L.; Yang, J.; Kosynkin, D. V.; Bronikowski, M. J.; Smalley, R. E.; Tour, J. M. Functionalization of Carbon Nanotubes by Electrochemical Reduction of Aryl Diazonium Salts: A Bucky Paper Electrode. *J. Am. Chem. Soc.* **2001**, *123*, 6536–6542.
- Bahr, J. L.; Tour, J. M. Highly Functionalized Carbon Nanotubes Using In Situ Generated Diazonium Compounds. *Chem. Mater.* **2001**, *13*, 3823–3824.
- Holzinger, M.; Vostrowsky, O.; Hirsch, A.; Hennrich, F.; Kappes, M.; Weiss, R.; Jellen, F. Sidewall Functionalization of Carbon Nanotubes. *Angew. Chem.* **2001**, *40*, 4002–4005.
- Georgakilas, V.; Kordatos, K.; Prato, M.; Guldi, D. M.; Holzinger, M.; Hirsch, A. Organic Functionalization of Carbon Nanotubes. *J. Am. Chem. Soc.* **2001**, *124*, 760–761.
- Thess, A.; Lee, R.; Nikolaev, P.; Dai, H.; Petit, P.; Robert, J.; Xu, C.; Lee, Y. H.; Kim, S. G.; Rinzler, A. G.; Colbert, D. T.; Scuseria, G. E.; Tomanek, D.; Fischer, J. E.; Smalley, R. E. Crystalline Ropes of Metallic Carbon Nanotubes. *Science* **1996**, *273*, 483–487.
- Rinzler, A. G.; Liu, J.; Dai, H.; Nikolaev, P.; Huffman, C. B.; Rodriguez-Macias, F. J.; Boul, P. J.; Liu, A. H.; Heymann, D.; Colbert, D. T.; Lee, R. S.; Fischer, J. E.; Rao, A. M.; Eklund, P. C.; Smalley, R. E. Large-Scale Purification of Single-Wall Carbon Nanotubes: Process, Product, and Characterization. *Appl. Phys. A* **1998**, *67*, 29–37.
- Nikolaev, P.; Bronikowski, M. J.; Bradley, R. K.; Rohmund, F.; Colbert, D. T.; Smith, K. A.; Smalley, R. E. Gas-Phase Catalytic Growth of Single-Walled Carbon Nanotubes from Carbon Monoxide. *Chem. Phys. Lett.* **1999**, *313*, 91–97.
- Bronikowski, M. J.; Willis, P. A.; Colbert, D. T.; Smith, K. A.; Smalley, R. E. Gas-Phase Production of Carbon Single-Walled Nanotubes from Carbon Monoxide via the HiPco process: A Parametric Study. *J. Vac. Sci. Technol. A* **2001**, *19*, 1800–1805.
- Lagow, R. J.; Badachape, R. B.; Wood, J. L.; Margrave, J. L. Some New Synthetic Approaches to Graphite-Fluorine Chemistry. *J. Chem. Soc., Dalton Trans.* **1974**, *12*, 1268–1273.
- (a) Mickelson, E. T.; Huffman, C. B.; Rinzler, A. G.; Smalley, R. E.; Hauge, R. H.; Margrave, J. L. Fluorination of Single-Wall Carbon Nanotubes. *Chem. Phys. Lett.* **1998**, *296*, 188–194. (b) Mickelson, E. T. Novel Chemistry of Elemental Carbon: Graphite, Fullerenes and Nanotubes. Ph.D. Thesis, Rice University, Houston, TX, 1999. (c) Chiang, I. W. Science of Single-Wall Carbon Nanotubes: Purification, Characterization and Chemistry. Ph.D. Thesis, Rice University, Houston, TX, 2001.
- Mickelson, E. T.; Chiang, I. W.; Zimmerman, J. L.; Boul, P. J.; Lozano, J.; Liu, J.; Smalley, R. E.; Hauge, R. H.; Margrave, J. L. Solvation of Fluorinated Single-Wall Carbon Nanotubes in Alcohol Solvents. *J. Phys. Chem. B* **1999**, *103*, 4318–4322.
- Dunitz, J. D.; Taylor, R. Organic Fluorine Hardly Ever Accepts Hydrogen Bonds. *Chem. Eur. J.* **1997**, *3*, 89–98.
- Kelly, K. F.; Chiang, I. W.; Mickelson, E. T.; Hauge, R. H.; Margrave, J. L.; Wang, X.; Scuseria, G. E.; Radloff, C.; Halas, N. J. Insight into the Mechanism of Sidewall Functionalization of Single-Walled Nanotubes: An STM Study. *Chem. Phys. Lett.* **1999**, *313*, 445–450.
- Kudun, K. N.; Bettinger, H. F.; Scuseria, G. E. Fluorinated Single-Wall Carbon Nanotubes. *Phys. Rev. B* **2001**, *63*, 45413–45421.
- Gu, Z.; Peng, H.; Hauge, R. H.; Smalley, R. E.; Margrave, J. L. Cutting Single-Wall Carbon Nanotubes through Fluorination. *NanoLett.* **2002**, *2*, 1009–1013.
- Chiang, I. W.; Brinson, B. E.; Huang, A. Y.; Willis, P. A.; Bronikowski, M. J.; Margrave, J. L.; Smalley, R. E.; Hauge, R. H. Purification and Characterization of Single-Wall Carbon Nanotubes (SWNTs) Obtained from the Gas-Phase Decomposition of CO (HiPco Process). *J. Phys. Chem. B* **2001**, *105*, 8297–8301.
- Taylor, R. Progress in Fullerene Fluorination. *Russ. Chem. Bull.* **1998**, *47*, 823–832.



- (32) Bettinger, H. F.; Kudin, K. N.; Scuseria, G. E. Thermochemistry of Fluorinated Single Wall Carbon Nanotubes. *J. Am. Chem. Soc.* **2001**, *123*, 12849–12856.
- (33) Saini, R. K.; Chiang, I. W.; Peng, H.; Smalley, R. E.; Billups, W. E.; Hauge, R. H.; Margrave, J. L. Covalent Sidewall Functionalization of Single Wall Carbon Nanotubes. *J. Am. Chem. Soc.* **2002**, in press.
- (34) Boul, P. J.; Liu, J.; Mickelson, E. T.; Huffman, C. B.; Ericson, L. M.; Chiang, I. W.; Smith, K. A.; Colbert, D. T.; Hauge, R. H.; Margrave, J. L.; Smalley, R. E. Reversible Sidewall Functionalization of Buckytubes. *Chem. Phys. Lett.* **1999**, *310*, 367–372.
- (35) Lobo, R.; Khabashesku, V. N.; Margrave, J. L. Unpublished results.
- (36) Stevens, J. L.; Huang, A. Y.; Chiang, I. W.; Khabashesku, V. N.; Margrave, J. L. Sidewall Aminoalkyl Functionalization of Single-Walled Carbon Nanotubes Using Fluoronanotube Precursors. *Angew. Chem., Int. Ed.* **2002**, in press
- (37) Tumanski, B. L. An ESR Study of Radical Reactions of C<sub>60</sub> and C<sub>70</sub>. *Russ. Chem. Bull.* **1996**, *45*, 2267–2278.
- (38) Peng, H.; Reverdy, P.; Khabashesku, V. N.; Margrave, J. L. Sidewall Functionalization of Single-Wall Carbon Nanotubes with Organic Peroxides. *Chem Commun.* **2002**, in press.
- (39) Peng, H.; Gu, Z.; Liu, Y.; Chiang, I. W.; Smalley, R. E.; Hauge, R. H.; Khabashesku, V. N.; Margrave, J. L. Oxidative Properties and Chemical Stability of Fluoronanotubes in Matrixes of Binary Inorganic Compounds. *J. Nanosci. Nanotech.* **2002**, in press.
- (40) Peng, H.; Gu, Z.; Yang, J.; Zimmerman, J. L.; Willis, P. A.; Bronikowski, M. J.; Smalley, R. E.; Hauge, R. H.; Margrave, J. L. Fluorotubes as Cathodes in Lithium Electrochemical Cells. *Nano-Lett.* **2001**, *1*, 625–629.

AR020146Y